Calculations of generalized dynamic structure factor for amorphous silicon

J. L. Feldman

Center for Computational Materials Science,

Naval Research Laboratory,

Washington, D.C. 20375-5345

(November 16, 2001)

Abstract

In an extension of previous studies of ours a normal mode analysis is performed for a 4096 atom structural model, of cubic cell size L=44$\mathring{A}$, of amorphous silicon within the Stillinger Weber potential. The peaks in dynamic structure factor quantities $S_L(Q,\omega)$ and $S_T(Q,\omega)$, where L and T refer to projections of eigenvectors onto vectors parallel and perpendicular to $\mathbf{Q}$, are compared with use of Lorentzian fits. An attempt is made to estimate Ioffe-Regel crossover frequencies. In agreement with a previous estimate for the commencement of diffusons a frequency corresponding to 17 meV is found for the transverse-like Ioffe-Regel crossover. S_L for fixed Q, is found to be reasonably Lorentzian up to Q=3 $(2\pi/L)$. S_L functions which have peak-height frequencies above the transverse acoustic maximum frequency $\omega_{T,max}$ are strongly skewed towards higher frequencies. The Lorentzian breadths above and below $\omega_{T,max}$ are roughly of the forms Q^2 and Q^4, respectively. Finally, a small positive dispersion describes the peak positions of S_L, in qualitative agreement with related studies on other model glassy systems.

I. INTRODUCTION

The dynamical properties of glasses at frequencies in the sub- and low-terahertz region have been investigated intensively. Both computer simulation [1–4] and experiment [1,5] suggest that elastic scattering gives rise to a Q^2 law for the breadths of phonon peaks in the dynamic structure factor as well as in a generalized quantity based on transverse polarization projections of normal mode eigenvectors. This law seems to be clearly observed experimentally (longitudinal projected) only in the nanometer region, and computer simulations have not been able to extend beyond that region. It is often assumed, e.g. [6,5], that at sufficiently low Q a Q^4 Rayleigh elastic scattering law will prevail. But a different theoretical approach indicates that the extension of the Q^2 elastic scattering law down to Q=0 [7] is conceivable. In addition there has been considerable discussion about the spectral shapes of the measured inelastic x-ray scattering for various glasses. Courtens et al. [5] argue for an effective medium like formula, and show analyses of data that support that, whereas Ruocco et al. argue for a Lorentzian behavior. In addition a hard sphere model calculation based on mode coupling theory [8] has reproduced some of the qualitative experimental findings.

In previous numerical investigations we have discussed the vibrational normal modes of amorphous silicon from the point of view of propogational and thermal conduction properties. [9] In particular we have described the modes by considering the localization-delocalization properties as well as phase coherency. The models indicate that both ordinary propagating modes and resonance modes coexist in the same low frequency region, that there exists delocalized but non propagating modes, and that localized modes exist at only the top few percent of the spectrum. Allen and Fabian [10] have named the modes propagons, diffusons and locons. In an earlier paper [4] we argued that our results did not imply the presence of resonance modes in macroscopic samples, unless they contained sufficient structural inhomogeneities. Nevertheless there is still some question about whether or not the Stillinger Weber potential leads to resonance modes in the absence of such inhomogeneities.

As done previously, we base our work on the Stillinger Weber potential. [11] Structural

models based on the WWW bond switching algorithm [12] were supplied by Wooten and subsequently "relaxed" via the Stillinger Weber potential as first done by Broughton and Li. [13]

II. FOURIER TRANSFORMS OF A FEW SELECTED EIGENVECTORS

Within our models the dynamic structure factor loses its phonon character at a frequency where modes are still extended throughout the computational box. [9] We consider this to be a well established result of present model calculations on several glassy systems. What we consider here in more detail and with better statistics than previously obtained is the extended and plane wave nature of the modes over the lower half of the frequency spectrum.

Before examining the dynamical structure factor it is instructive to consider $C_{i,1}$ and $C_{i,2}+C_{i,3}$, for a few selected modes, where

$$C_{i,\alpha} = <\mid \sum_l \mathbf{e}_i(l).\mathbf{n}_{\alpha,\mathbf{Q}} exp(i\mathbf{Q}\cdot\mathbf{r}_l) \mid^2> \qquad (1)$$

In Eq. 1 the brackets imply an average over all $\mathbf{Q}$ of fixed magnitude. (We also restrict $\mathbf{Q}$ to be consistent with the periodic boundary conditions). Further, $\mathbf{e}_i$ is the eigenvector associated with the i'th normal mode, $\mathbf{r}_l$ is an atomic position vector, and the $\mathbf{n}_{\alpha,\mathbf{Q}}$ (α=1-3) are orthogonal unit vectors parallel ($\alpha = 1$) and perpendicular (α=2,3) to $\mathbf{Q}$. The modes represented in Figs. 1 and 2 correspond to frequencies slightly less than and significantly above $\omega_{TA,max}$, respectively, where $\omega_{TA,max}$ is defined as the frequency above which a Q corresponding to transverse acoustic projection is not definable. In the vibrational density of states, presented for our model in earlier papers, e.g. [4], this frequency occurs near the lowest frequency peak height. The extremely broad distribution of the transverse Fourier content shown in Fig. 1 of course implies $\omega_{TA,max} \approx 22.3$ meV. Fig. 2 also illustrates the idiosynchratic character of the individual modes, although variations among modes of adjacent frequencies is smaller than that of the longitudinal projected quantities seen in the figure. For the purpose of comparison we also present the static structure factor, F^2, for our model (Fig. 1).

III. RESULTS FOR DYNAMIC STRUCTURE FACTOR

The (intermediate) dynamic structure factor, $S_L(Q,\omega)$, is defined as $\sum_i C_{i,1}\delta(\omega_i-\omega)$ with a similar expression involving the sum of two terms for S_T. In a previous paper [9] on a 1000 atom model of the same type as we employ here for 4096 atoms we plotted results for an S_L defined for individual **Q**'s, mainly along the 100 direction. It is therefore encouraging that those results are consistent with the results to be given here. Previously we also reported directionally averaged results for our 4096 atom model, but those corresponded only to transverse projections of eigenvectors and to $Q \leq 2.236$ (Q is in units of $2\pi/L$ where L (= 44 $\AA$) is the size of the cubic spercell). [4]

First we give some results for the transverse projected dynamic structure factor to complete our earlier study. Figure 3 shows only results higher in Q than we considered before. The dashed lines represent Lorentzian fits to the results and the inset gives the Lorenzian peak position and HWHM as a function of Q. The dashed and dotted lines in the inset are not fits to the present results but rather the formulas found to represent the earlier low Q results. They show that a quadratic linewidth as a function of Q is an excellent representation of the results up to Q/Q_0=0.45 and that negative dispersion is evident slightly beyond Q/Q_0=0.36 where Q_0 is the position of the first peak in the static structure factor. The crossing of the two curves at $\omega = 17meV$ is the Ioffe-Regel crossover (discussed in more detail below) for transverse modes. This value is in excellent agreement with a previous estimate for the onset of diffusons. [18]

Figure 4 gives the proper dynamic structure factor, i.e., the longitudinal projection, aside from Debye Waller factor and non vibrational constants, for selected values of Q. There is a dramatic change in the character of $S(Q,\omega)$ at Q = 3.5 as seen in Fig.5, and figure 6 shows results for Q> 3.5. The low Q results seem to be well represented by Lorentzians. This is true for transverse projected results as well. [4] (On the other hand it is interesting to point out that Lorentzians do not represent $S(Q,\omega)$ for a similar structural model but with use of a Keating potential model [14]). At $\omega_{TA,max}$, "transverse mode" cutoff the peaks change in

character as they become clearly skewed to high frequencies.

The peak position corresponding to the Lorentzian fits displayed in the previous figures are plotted in Fig. 7. (Also plotted are results for a few values of Q which we have not given in any additional detail.) The straight line in Fig. 7 is a fit to the lowest four points. It is given by the equation $\omega = 7.13Q$ where ω is in meV and Q in $2\pi/L$. The corresponding sound velocity is 7.59X10^{3}m/s in excellent agreement with a determination of 7.64X10^{3}m/s, quoted in the second reference of [9] based on a determination of elastic constants for a 1000 atom model using the method of long waves. [15]. There is clear evidence of a positive curvature in the dispersion. Positive dispersion was also noticed in other simulational studies. [2,3] In the present work, as well as possibly in others', the onset of positive dispersion seems to occur near the (transverse polarization) Ioffe-Regel crossover.

Just above $\omega_{T,max}$ we obtain a dramatic decrease in the above Lorentzian character (propagon weight) as also seen in Fig. 7. We define propagon weight here as the fraction of the total area under a fitted Lorentzian to the total area under S(Qω) which is a constant, independent of Q, by virtue of the known sum rule. Of course this quantity should be less than one even for highly propagating states because of the "internal displacements" present due to optic like mode-elastic wave harmonic interaction terms.

The Ioffe-Regel crossover has been considered for these systems with somewhat varying definitions. In Fig. 8, e.g., we allude to the definition also used by Taraskin et al. [16] in which the lifetime associated with phase decoherence is equated to the frequency. [17] The frequency is greater than the HWHM of S(Q,ω) for the plotted quantities, suggesting that the Ioffe-Regel criterion for propagating states is satisfied. However, the fact that S(Q,ω) is greatly skewed suggests otherwise. The forms that approximate the low and high frequency Lorentzian fits are $\Gamma/2 = 0.3Q^2$ and $\Gamma/2 = 0.002Q^4$, respectively, where the same units as above are employed.

We do not show S_L for Q above 6.4, although we have performed calculations for Q=7 and Q=8 and find that a Lorentzian gives an extremely poor fit to the results. These Q's are beyond $Q_0/2$, where Q_0 is the position of the first maximum in the structure factor.

Fourier contents of modes are also indirectly related to the phase quotient definition, so that as modes contain greater wave vector components beyond certain wave numbers they also tend to yield negative phase quotients. Such a correlation is evident by comparing behavior shown in Fig. 13 of Ref. [18] with results of the present investigation.

Fig. 2 illustrates that individual modes are sharp with respect to Q and longitudinal acoustic polarization. But this sharpness is not inconsistent with the fact that S(Q,ω) is strongly skewed as a function of ω, for higher frequency modes give broader FT's and are denser in frequency space. In the context of the Kubo theory of thermal conductivity, the diffusivity function is peaked in the 'longitudinal acoustic' frequency region [9,4] but the contribution to the thermal conductivity from a given frequency region can be expected to be smaller than what it would be if the modes were good propagating modes.

IV. CONCLUSIONS

We have performed a Fourier-like analysis of modes in a 4096 atom model to glean information on the propagational nature of the modes in a continuing study of this basic model. The nature of the longitudinal projected quantities is similar to that in other studies in some respects and dissimilar in others. As in other studies we find that there is a positive dispersion of the longitudinal branch initially and then there is the usual negative dispersion at higher frequencies. The onset of this positive dispersion seems to be approximately associated with the Ioffe-Regel crossover for transverse polarization. Such a correspondence has not been noted in studies on other models, and it would be interesting to explore this point further. Apparently unlike other simulations, the Lorentzian weight is greatly reduced and yet the peaks are in some sense sharpened as one goes through this maximum transverse acoustic frequency. We have determined a clear Ioffe-Regel crossover of 17 meV, based on the transverse projected quantities, and probably the Ioffe-Regel crossover for longitudinal polarization should be taken to be approximately 25 meV.

V. ACKNOWLEDGMENTS

I am grateful to William Garber and Folkert Tangerman for the diagonalization of the dynamical matrix using the galaxy cluster at SUNY at Stony Brook. I am also grateful to Philip Allen for sharing his insights about the nature of the vibrational modes in glasses.

REFERENCES

[1] Dell'Anna, R., Ruocco, G., Sampoli, M., and Viliani, G., 1998, Phys. Rev. Lett. **80**, 1236.

[2] Horback, J., Kob, W., and Binder, K., 2001, Euro. Phys. J. B **19**, 531.

[3] Ruocco, G., Sette, F., Leonardo, R.D., Monaco, G., Sampoli, M., Scopigno, T., and Viliani, G., 2000, Phys. Rev. Lett. **84**, 5788.

[4] Feldman, J.L., Allen, P.B., and Bickham S. R., 1999, Phys. Rev. **59**, 3551.

[5] Courtens E., Foret, M., Hehlen B., and Vacher, R., 2001, Solid State Commun. **117**, 187, and references therein.

[6] Sokolov, A.P., Calemczuk, R., Salce, B., Kisliuk, A., Quitmann, D., and Duval, E., 1997, Phys. Rev. Lett. **78**, 2405.

[7] Martin-Mayor, V., Mezard, M., Parisi, G., and Verroccio, P., 2001, J. Chem. Phys. **114**, 8068.

[8] Gotze, W. and Mayr, M.R., 2000, Phys. Rev. E **61**, 587.

[9] Allen, P.B., and Feldman, J.L., 1993, Phys. Rev. B **48**, 12581.; Feldman, J.L., Allen, P.B., Kluge, M.D., and Wooten, F., 1993, Phys. Rev. B **48**, 12589.

[10] Fabian J. and Allen P.B., 1997, Phys. Rev. Lett. **79**, 1885.

[11] Stillinger, F.H., and T. A. Weber, T.A., 1985, Phys. Rev. B **31**, 5262 (1985).

[12] Wooten, F., Winer, K., and Weaire, D., 1985, Phys. Rev. Lett. **54**, 1392.

[13] Broughton, J.Q. and Li, X.P., 1987, Phys. Rev. B **35**, 9120.

[14] Feldman, J.L., Viliani, G., Garber, W., Tangerman, F.W., and Hellberg, C.S., 2001, Phil. Mag. B (in print).

[15] Feldman, J.L., Broughton, J.Q., and Wooten, F., 1991, Phys. Rev. B **43**, 2152.

[16] Taraskin, S.N. and Elliott, S.R., (2000-II), Phys. Rev. B **61**, 12031; ibid., 12017.

[17] The definition used in Ref. [9] is inappropriate as it is based on the lifetime associated with the number of phonons. Nevertheless this was not used in determining the onset of diffusons in Fig. 2 of Ref. [18] for the results of transverse S(Q,ω) of the present study also yields 17 meV for the onset of diffusons. Nevertheless the longitudinal "modes" appear to have a sharper dynamic structure factor peak than the transverse ones at identical peak frequencies leading to perhaps a higher frequency (approximately 25 meV) for which they can no longer be considered propagons, or, in the language of others [5], where strong scattering sets in.

[18] Allen, P.B., Feldman, J.L., Fabian J., and Wooten, F., 1999, Phil. Mag. B **79**, 1715.

VI. FIGURE CAPTIONS

Fig. 1. Longitudinal and Transverse Fourier components for mode at ω=22.3 meV. Also shown is the static structure factor, F^2 in arbitrary units. Q is in units of $2\pi/L$ in this and all succeeding figures.

Fig. 2. Longitudinal and Transverse Fourier components for modes at 38.3 and 38.7 meV (smaller height of longitudinal peak). T curves are shifted up by 0.3.

Fig. 3. Transverse dynamic structure factor results (solid) and Lorentzian fits (dashed). Inset shows values of peak heights and HWHM of Lorentzian fits. The values of Q for the peaks are 4, 5, 6, and 6.4.

Fig. 4. $S_L(Q,\omega)$ for $\mathbf{Q}$=(l,m,n) averaged over all permutations of l,m,n. Dashed curves are Lorentzian fits.

Fig. 5. $S_L(Q,\omega)$ for various values of Q. Dashed curves are Lorentzian fits. Fit to Q=3.6 result is made only for limited (right) portion including the peak height.

Fig. 6. Same as Fig. 5 caption.

Fig. 7. Phonon energy (stars) and propagon weight (plusses). The propagon weight is defined as the area under the Lorentzian fits to the curves in Figs. 4-6. The phonon energies are also taken from those Lorentzian fits. The dotted line is a fit to $v_L Q$ at low Q.

Fig. 8. The halfwidths (plusses) of the Lorentzian fits of the Figs. 4-6. For comparison based on a definition of the Ioffe-Regel crossover the phonon energies are also given. The straight line going through the latter curve corresponds to $v_L Q$ and the other two straight lines are Q^2 and Q^4, where the former is seen to approximate the low Q results and the latter the high Q results.

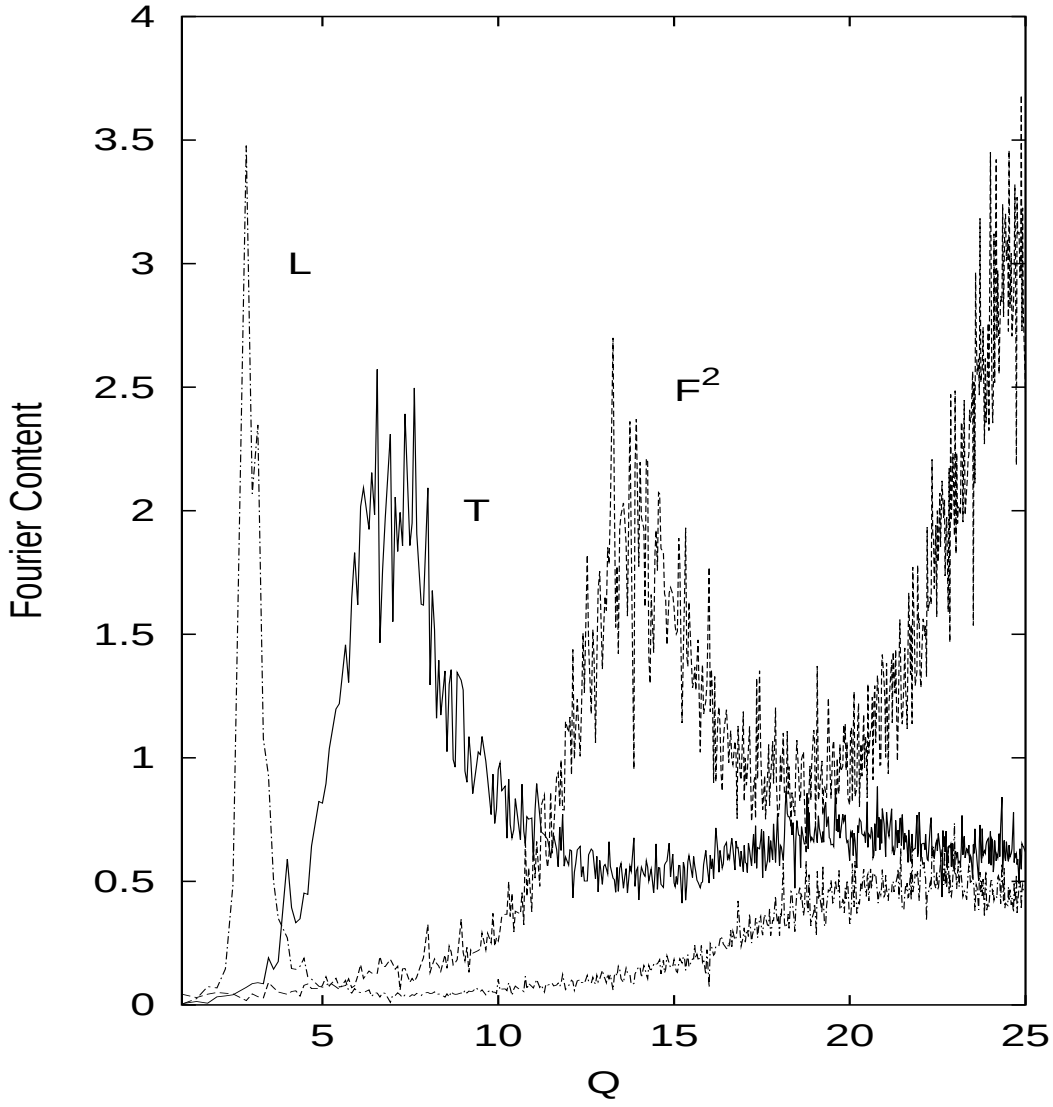

FIG. 1.

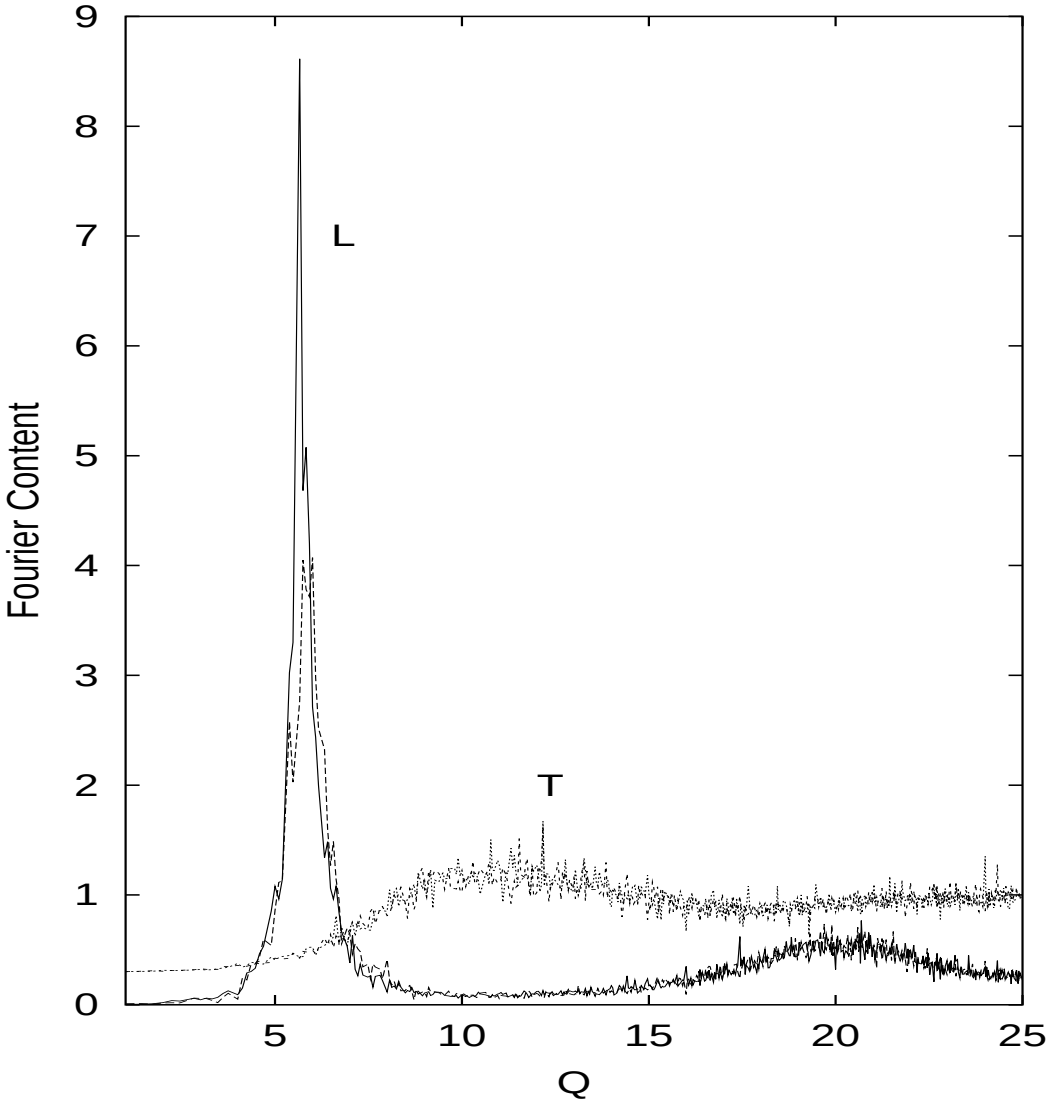

FIG. 2.

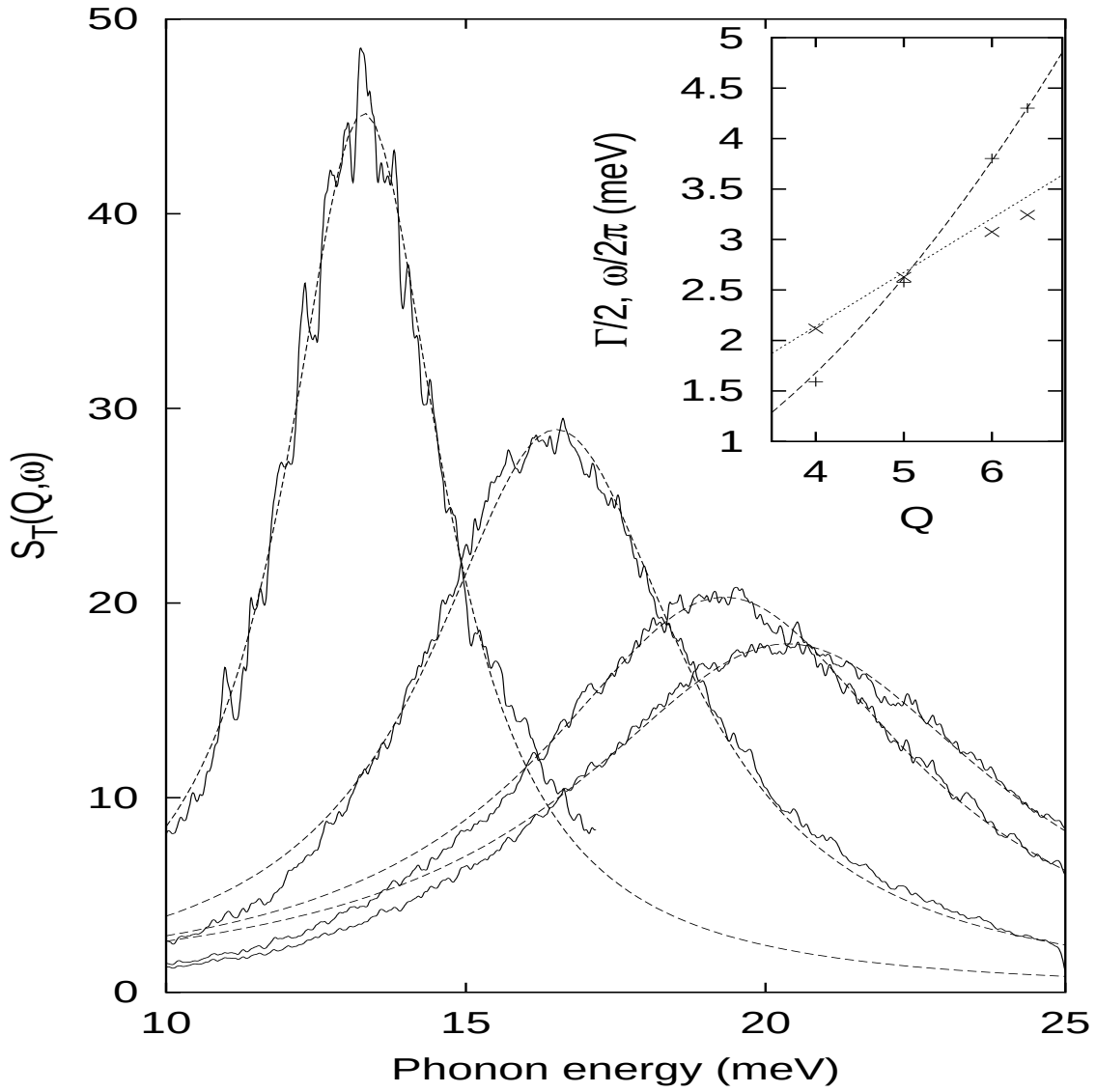
50
40
30
20
10
0
10
15
20
25
Phonon energy (meV)
$S_T(Q,\omega)$
5
4.5
4
3.5
3
2.5
2
1.5
1
4
5
6
Q
$\Gamma/2,\ \omega/2\pi$ (meV)

FIG. 3.

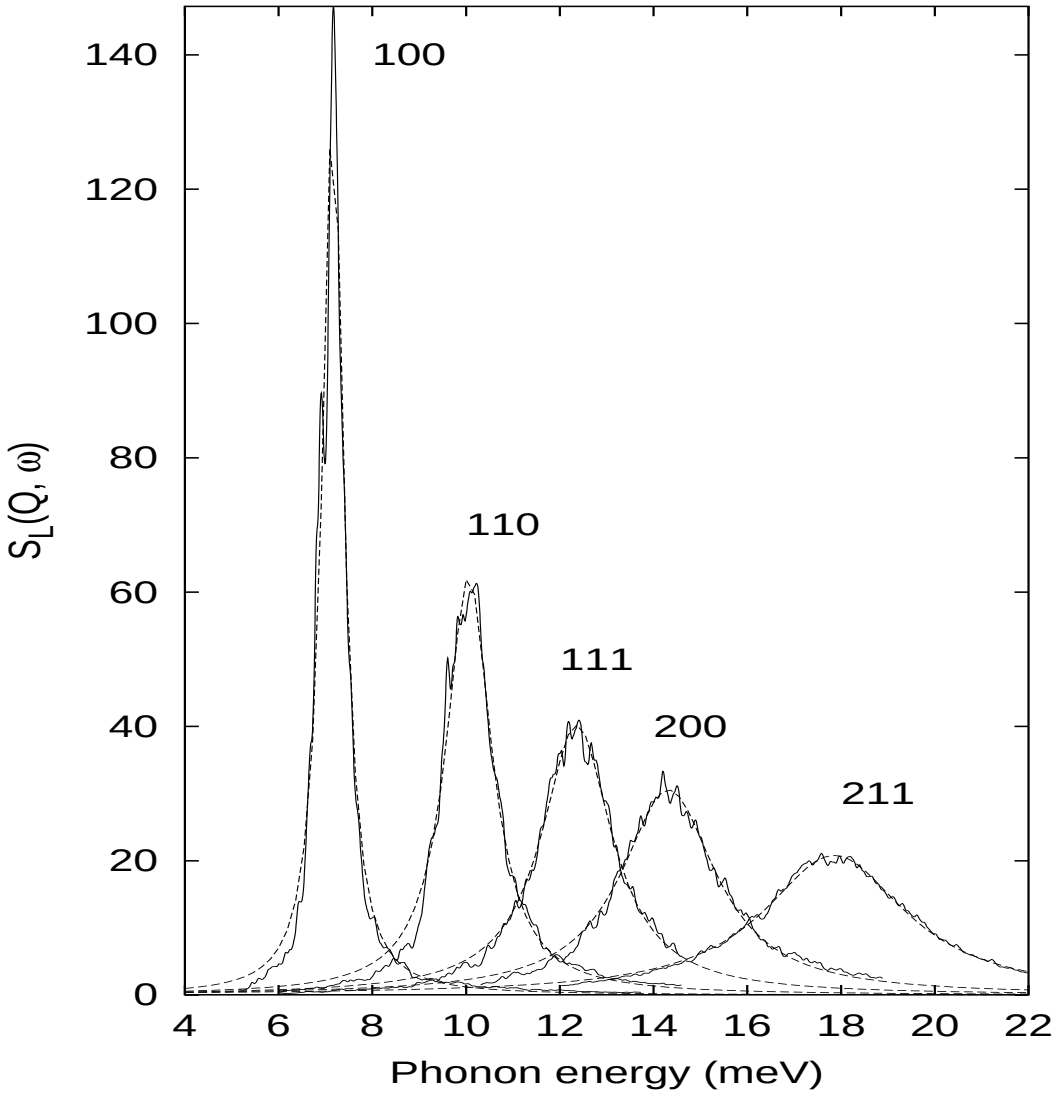
140
120
100
80
60
40
20
0
$S_L(Q,\omega)$
100
110
111
200
211
4
6
8
10
12
14
16
18
20
22
Phonon energy (meV)

FIG. 4.

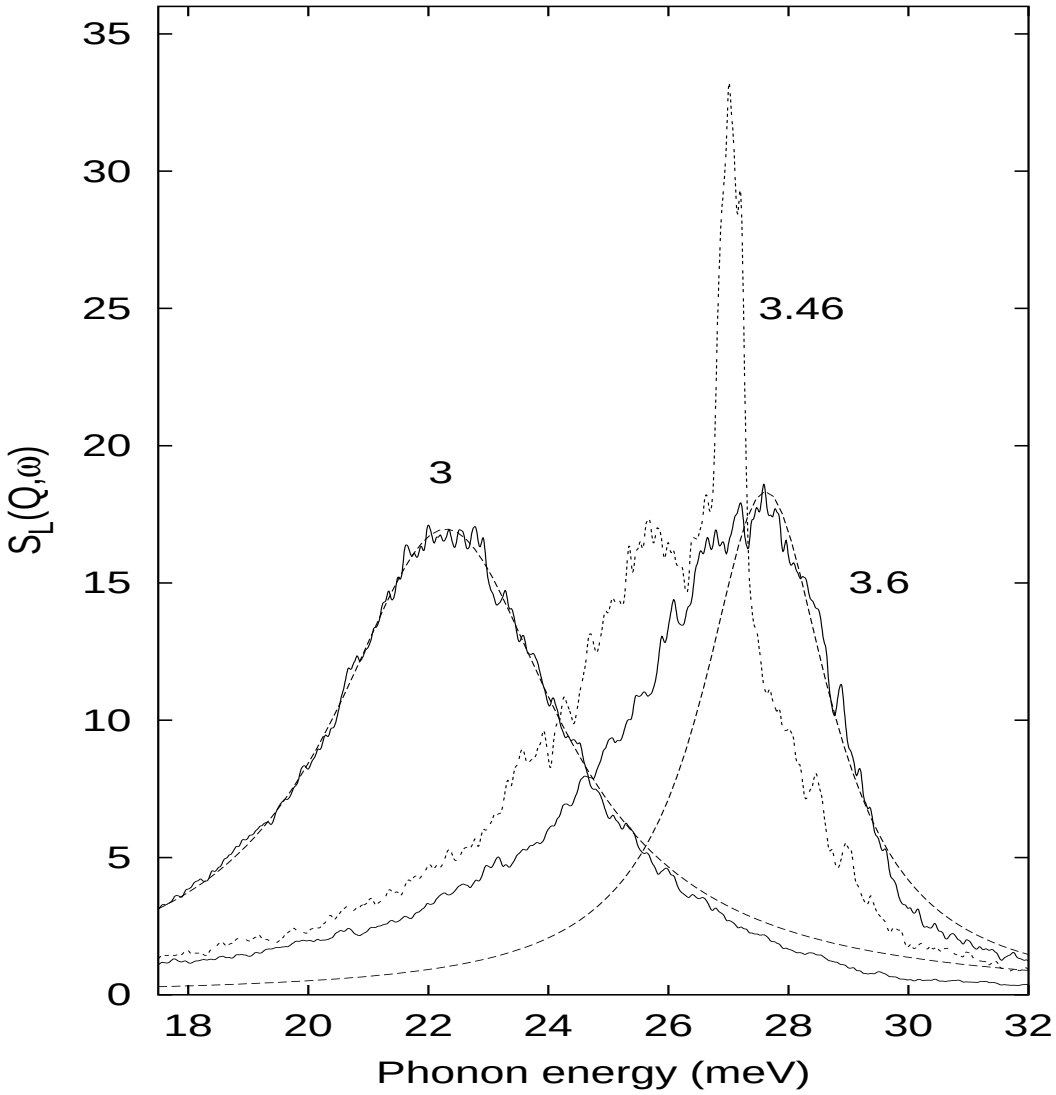
35
30
25
20
15
10
5
0
18
20
22
24
26
28
30
32
$S_L(Q,\omega)$
Phonon energy (meV)
3
3.46
3.6

FIG. 5.

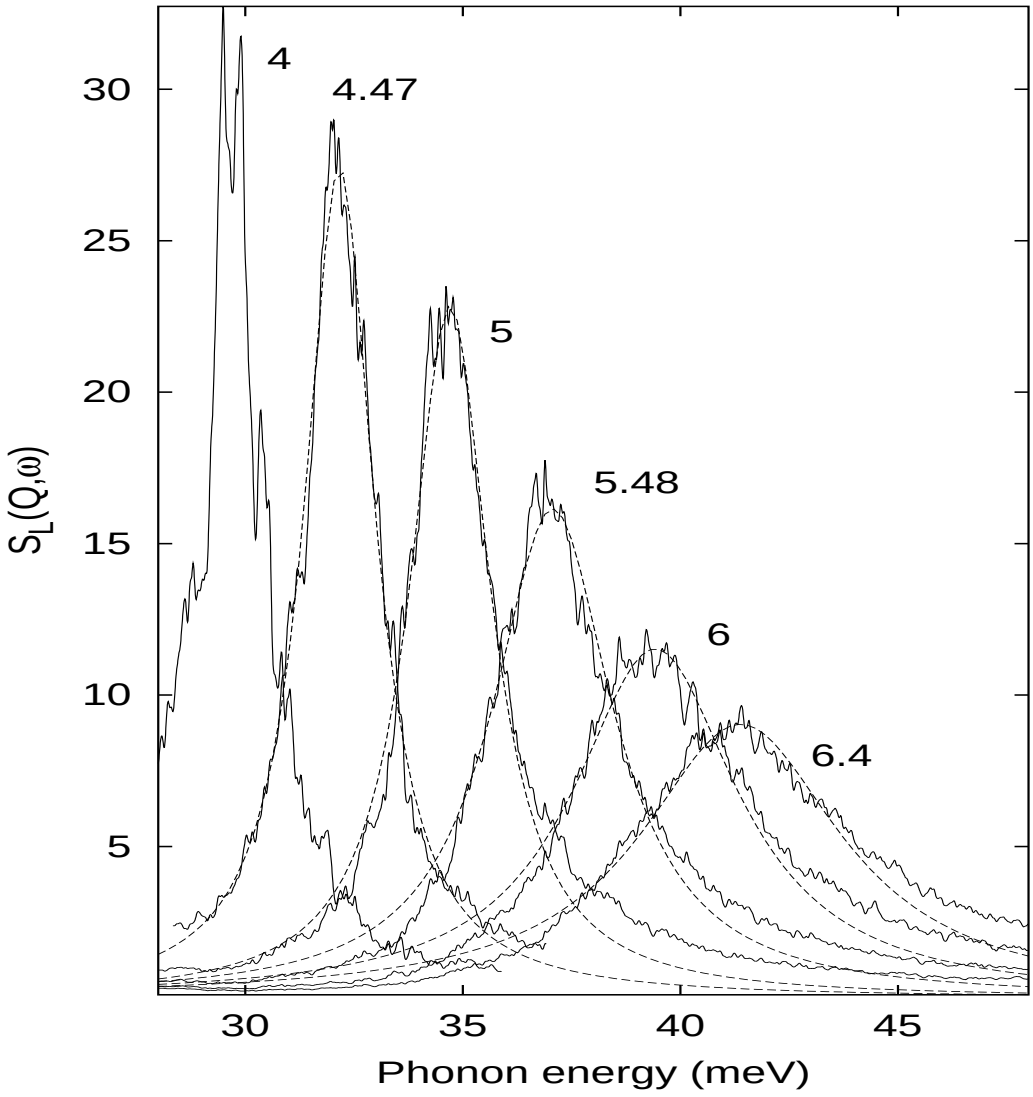
4
4.47
5
5.48
6
6.4
30
25
20
15
10
5
30
35
40
45
$S_L(Q,\omega)$
Phonon energy (meV)

FIG. 6.

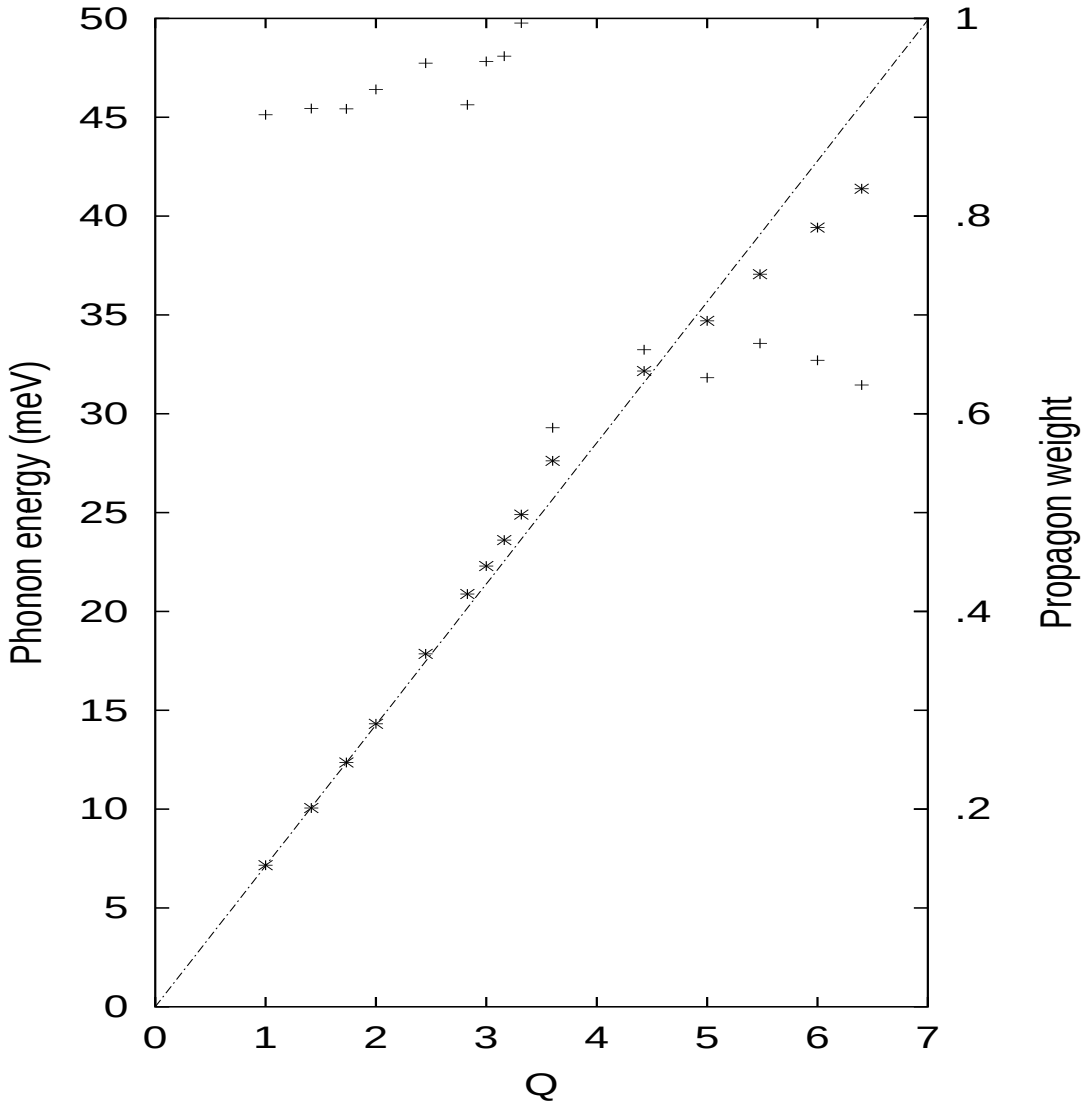
Phonon energy (meV)
Propagon weight
Q
0
5
10
15
20
25
30
35
40
45
50
.2
.4
.6
.8
1
0
1
2
3
4
5
6
7

FIG. 7.

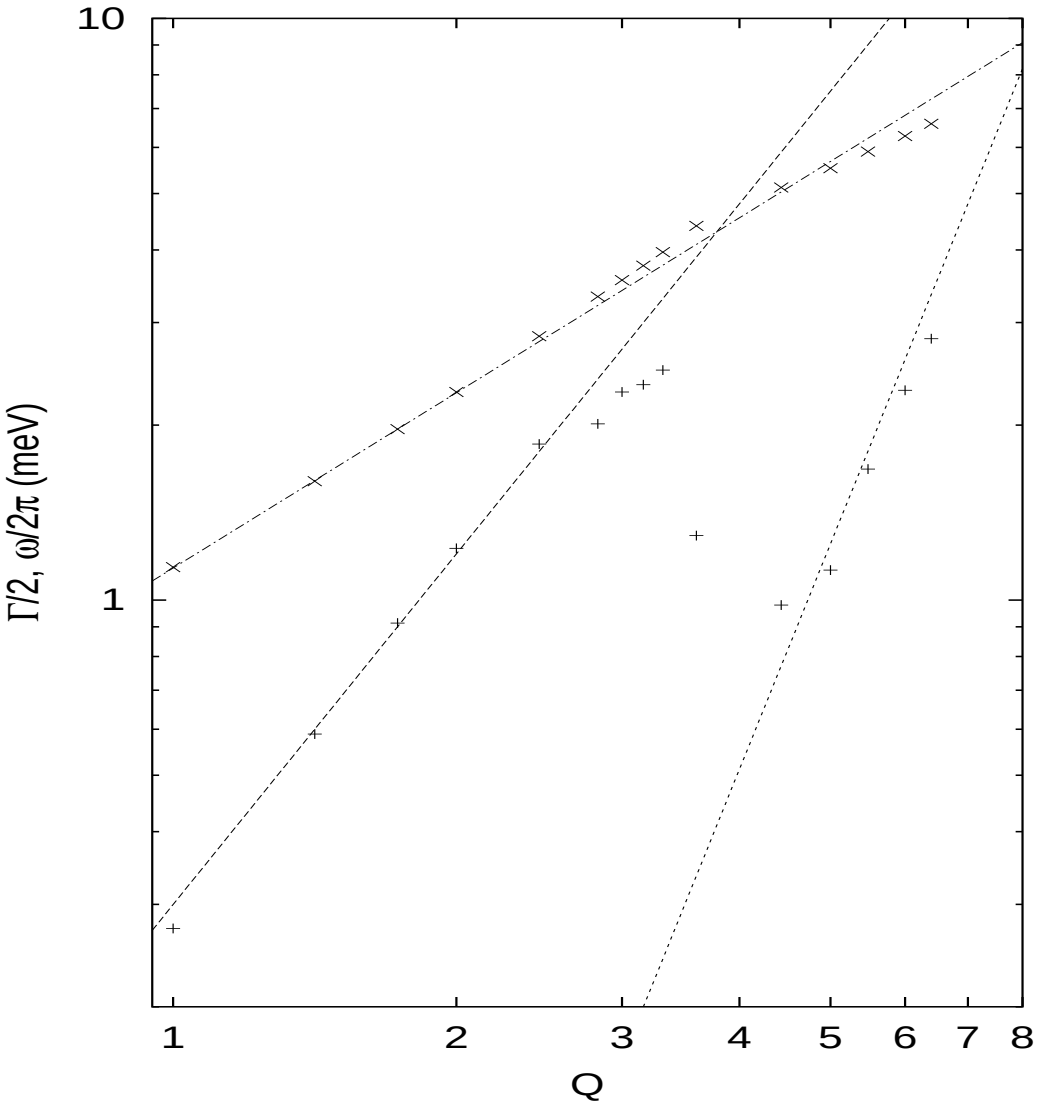

FIG. 8.